Fuzzy sets on 2D spaces for fineness representation

Jesús Chamorro-Martínez and Pedro Manuel Martínez-Jiménez
Department of Computer Science and Artificial Intelligence
University of Granada, Spain

José Manuel Soto-Hidalgo
Department of Computer Architecture, Electronics
and Electronic Technology, University of Córdoba, Spain

Belén Prados-Suárez
Department of Software Engineering, University of Granada, Spain

This is the peer reviewed version of the following article: *Jesús Chamorro-Martínez, Pedro Manuel Martínez-Jiménez, José Manuel Soto-Hidalgo, Belén Prados-Suárez: Fuzzy sets on 2D spaces for fineness representation. Int. J. Approx. Reasoning 62: 46-60 (2015)*, which has been published in final form at https://doi.org/10.1016/j.ijar.2015.05.005.

Abstract

The analysis of the perceptual properties of texture plays a fundamental role in tasks like semantic description of images, content-based image retrieval using linguistic queries, or expert systems design based on low level visual features. In this paper, we propose a methodology to model texture properties by means of fuzzy sets defined on bidimensional spaces. In particular, we have focused our study on the fineness property, that is considered as the most important feature for human visual interpretation. In our approach, pairwise combinations of fineness measures are used as reference set, which allows to improve the ability to capture the presence of this property. To obtain the membership functions, we propose to learn the relationship between the computational values given by the measures and the human perception of fineness. The performance of each fuzzy set is analyzed and tested with the human assessments, allowing us to evaluate the goodness of each model and to identify the most suitable combination of measures for representing the fineness presence.

Keywords: fuzzy sets; feature extraction; image analysis; texture modelling; human perception

1 Introduction

Texture is, together with color and shape, one of the most used features for image analysis and, in addition, one of the most difficult to characterize due to its imprecision. In fact, there is not an accurate definition for the concept of texture, but some widespread intuitive ideas. In this way, texture is described by some authors as local changes in the intensity patterns or gray tones which is used in opposition to the homogeneity idea [1]. Other authors consider texture as a set of basic items called *texels* (or texture primitives), arranged in a certain way [2]. However, for humans, the most common way to describe texture is by using vague textural properties, like *coarseness*, *directionality* or *regularity* [3, 4], that give them an informal way to represent their perception about these texels. Thus, coarseness is related to the spatial size of texture primitives, directionality reflects whether they have a dominant orientation, and regularity refers to the variation of their placement.

In this sense, the wide variety of techniques proposed in the literature to describe texture can be classified into two main approaches. In the first one, textures are modelled by means of feature vectors (that usually have very large dimensions) which have no direct relationship with the different perceptual properties. This approach does not provide a textural representation interpretable by humans but it allows to compare different textures on the basis of the similarity between its feature vectors. Most of these techniques are based on multiresolution analysis and scale-space theory, such as Gabor functions [5, 6, 7, 8] or Wavelets [9, 10, 11], that are considered as the golden standard in the literature. These approaches are applied in some classical tasks like texture segmentation [12, 13, 14] and classification [15, 16, 17], or in content-based image retrieval using query by image example [6, 18, 19]. Moreover, they can be used in texture synthesis techniques [20, 21, 22].

The second approach that can be found in the literature to describe texture includes the techniques that propose a texture characterization based on its perceptual properties, i.e. the descriptors obtained with these models have a direct relationship with the textural properties. Such techniques are very useful in tasks where some interaction with users is needed, as they try to describe texture in a similar way as humans would. Thus, in addition to the classical tasks commented above, this type of techniques can also be applied in fields such as semantic description of images [23, 24, 25] or in content-based image retrieval using linguistic queries [26, 27, 28].

Focusing our attention on this second group of techniques, we can find in the literature many measures that, given an image, capture the presence of a textural property in the sense that the greater the value given by the measure, the greater (lower) the presence of this property [4, 29, 30, 31, 32]. However, the direct use of these computational measures in the analysis of the perceptual properties raises several problems. The first one is related with the election of the most suitable measure. There is a large number of computational measures associated with each property, but no comparative studies can be found in the literature that analyze the ability of each measure to capture the corresponding

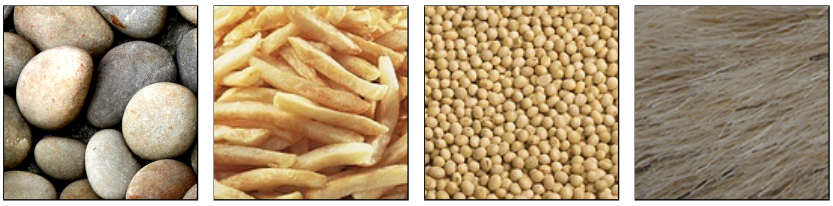

(a) (b) (c) (d)

Figure 1: Examples showing the imprecision associated to the texture properties.

property. Regardless what measures are used, another problem is related to the own imprecision associated to the perceptual properties. This imprecision must be understood in the sense that, except in extreme cases, we cannot set a precise threshold between textures that accomplish strictly a property and textures that do not, but it is possible to indicate the more or less accomplishment of the property in the texture. For example, we can safely say that the texture shown in Figure 1(a) is coarse and contrasted, and that the texture shown in Figure 1(d) is not, as they represent extreme cases for both properties. However, the accomplishment of these properties is not so clear for the textures shown in figures 1(b) and 1(c). Although this imprecision suggests the use of representation models that incorporate the uncertainty associated to the properties, all the measures commented above are crisp proposals, which do not model any kind of imprecision.

For facing the imprecision problem, some proposals arise from the fuzzy set field [33, 34], and more specifically from the content-based image retrieval area, where semantic data and imprecision related to texture are managed by means of fuzzy sets [26, 28, 35, 36, 37]. In these proposals, a mapping from low-level statistical features (the crisp measures described above) to high level textural concepts is performed by defining membership functions for each textural feature. In most of these proposals, the measures used as reference set are associated with the coarseness property, that is the most popular one, being considered as the most fundamental feature in texture analysis by some authors [28]. In fact, the presence of fineness, that is the opposite concept to coarseness, is usually associated to the presence of texture (from this point of view, texture is defined as local variations against the idea of homogeneity). With regard to the membership functions, most of these fuzzy approaches propose to model the fineness property by means of fuzzy partitions providing a set of linguistic terms. In general, the fineness measure proposed by Tamura *et al.* in [4] is usually employed as reference set, and a fuzzy partition with five linguistic terms is obtained in the majority of the fuzzy approaches. This fuzzy partition is generated through an unsupervised fuzzy clustering algorithm on the basis of the measure values obtained from an image database.

However, all these fuzzy approaches have three main drawbacks, that from our knowledge have not been faced in the literature. First of all, the use of membership functions with a fixed form (usually triangles or trapezoids), prevents an accurate modelling of the textural concepts, allowing us to set only support and kernel limits. Moreover, linear functions are used for transitions, although it is known [38] that computational measures do not have a linear variation with the presence degree of the property. Second, the parameters that define these functions are adjusted manually or by using a fuzzy clustering, but without considering the relationship between the measure values and the human perception of the property. This implies that the obtained membership degrees do not necessarily match what a human would expect. And finally, these fuzzy approaches do not propose a global modelling of the textural concept, but a fuzzy partition providing a set of linguistic terms associated to this concept. This type of solution is unsuitable for some classical tasks, like pattern recognition, because a single presence degree of the textural property cannot be obtained, but one membership degree for each linguistic term in the partition.

In order to solve these problems, preliminary studies about the modelling of the fineness property have been presented in our previous work [39]. In that approach, the concept of texture has been modelled by means of a unique fuzzy set defined on the domain of computational texture measures. By considering the direct association between texture presence and fineness presence commented above, representative fineness measures have been used as reference set, i.e. we propose to model the concept of texture by representing its fineness presence. The use a unique fuzzy set instead of using a fuzzy partition allows to model the texture concept as a whole, which provides intuitive and very useful results, as it will be shown in section 6. In order to define the fuzzy set, parametric polynomial functions are proposed. Unlike triangular and trapezoidal ones, this type of functions allows to introduce more degrees of freedom to represent the variations in the presence degree, obtaining accurate models for the fineness property. Moreover, we propose to obtain the parameters of the membership function by considering the human perception of this property. To do this, a functional relationship between the computational values given by the measures and the human perception of fineness will be learned. To get information about the human perception, a set of images covering different presence degrees of fineness will be used to collect, by means of polls, human assessments from a set of subjects. This way, the presence degree given by the obtained fuzzy set will match what a human would expect.

However, in these preliminary studies only one crisp measure is used as reference set, which implies that only the ability of this measure to capture the corresponding property is considered in the modelling, although it is widely known that the combination of different measures improves the texture characterization [40]. In this paper we propose a perception-based fuzzy approach for texture modelling that extends these preliminary studies by considering the use of subsets of measures as reference set instead of using them individually. This new proposal allows to combine the ability of the different measures to capture the fineness presence, obtaining models that represent with more fidelity this

property, as it will be shown in section 5. In addition, the proposed approach allows us to address the first problem described above regarding the use of the computational measures, i.e. the election of the most suitable ones. In this paper, a group of fineness measures will be used, obtaining fuzzy sets defined on the domain of each measure separately as well as fuzzy sets defined on the domain of a combination of measures. In order to analyze the ability of each fuzzy set to represent the fineness property, goodness measures will be proposed taking into account the human assessments extracted from the poll. First, a ranking of individual measures will be obtained, allowing us to analyze each measure separately and to identify the most appropriate one. Second, a ranking of subsets of measures will be achieved, that will be used to identify the most suitable combination of measures. Moreover, comparing both rankings, we can verify that the combination of measures improves the fineness characterization.

The rest of the paper is organized as follows. In section 2 a general overview of our methodology is presented, introducing some basic concepts and the notation used in the paper. After that, the different elements of the model are described in detail in the following sections; specifically, the computational measures used as reference set are summarized in section 3, the way to obtain human assessments about the perception of fineness is faced in section 4, while section 5 describes the method employed to obtain the membership functions of the proposed fuzzy sets. In section 6 a comparative study of these models with the state of the art and some results obtained by applying them are shown. Finally, section 7 summarizes the main conclusions and future works.

2 Preliminaries and Notations

As mentioned in the above section, among all the perceptual texture properties, the *coarseness-fineness* is considered as the most fundamental one, being usually associated to the presence of texture. In this sense, a *fine* texture contains small texture primitives with large gray tone differences between neighbor pixels (e.g. the first image of Figure 2(a)), whereas a *coarse* texture corresponds to larger primitives formed by several pixels (e.g. the last image of Figure 2(a)). We can find in the literature many measures that, given an image, capture the fineness presence in the sense that the greater the value given by the measure, the larger (smaller) the texture primitives. In this paper we propose to model the concept of "texture" as a fuzzy set $\mathcal{T}_{\mathcal{F}}$ defined on the domain of a given subset $\mathcal{F}$ of fineness measures (our reference set). Note that, in general, a fineness measure takes values in $\mathbb{R}$, so the domain of our fuzzy set is $\mathbb{R}^{K'}$, with K' being the cardinality of $\mathcal{F}$. The membership function of this fuzzy set will be defined as[1]

$$\mathcal{T}_{\mathcal{F}} : \mathbb{R}^{K'} \rightarrow [0, 1] \tag{1}$$

For this modelling, two questions need to be faced: (i) what reference set should be used for the fuzzy set, and (ii) how to obtain the related membership

[1]To simplify the notation, as it is usual in the scope of fuzzy sets, we will use the same notation $\mathcal{T}_{\mathcal{F}}$ for the fuzzy set and for the membership function that defines it.

function. Concerning to the reference set, as mentioned above, we will define the fuzzy set on the domain of a given subset of fineness measures. Let $\mathbb{F} = \{F_1, \ldots, F_K\}$ be the set of K fineness measures used in this paper. From now on, we will denote by $\mathcal{F} \subseteq \mathbb{F}$ the subset of $K' \leq K$ measures selected from $\mathbb{F}$ to define the reference set. The measures analyzed in this paper, that include classical statistical measures, frequency domain approaches, fractal dimension analysis, etc., are summarized in section 3. All of them are automatically computed from the texture images.

With regard to the membership function, we propose to obtain it by using a perceptually-based approach that relates the fineness measures with the human perception of the property. For this purpose, two questions need to be faced: firstly, how to obtain the data about the "human perception" of fineness and, secondly, how to fit these data with the measures in order to obtain the membership function. To get information about the human perception of fineness, a set of images covering different presence degrees of this property has been gathered. This images are used to collect, by means of a poll, human assessments about the perceived fineness presence. From now on, let $\mathcal{I} = \{I_1, \ldots, I_N\}$ be the set of N images representing fineness examples, and let $\Gamma = \{v_1, \ldots, v_N\}$ be the set of fineness values associated to $\mathcal{I}$, with v_i being the value representing the degree of fineness perceived by humans in the image $I_i \in \mathcal{I}$. The description of the texture image set and the way to obtain Γ are detailed in section 4.

To obtain the membership function $\mathcal{T}_{\mathcal{F}}$ for a given subset of measures $\mathcal{F} \subseteq \mathbb{F}$, a robust fitting method is employed in order to represent the relationship between the values obtained by applying the measures in $\mathcal{F}$ to each image, and the degree of fineness perceived by humans in these images. This fitting method is described in section 5.

3 Fineness Measures: the Reference Set

In this paper, we have initially considered the 17 fineness measures analyzed in our previous work [38]. These measures can be classified into 3 groups according to the strategy used to quantify the coarseness of the texture image. The first group includes those measures that try to estimate directly the size of the texels by analyzing the pixels of the image. In this group we can find the measure defined by Abbadeni *et al.* in [31], the measure proposed by Tamura *et al.* in [4], the Edge Density (ED measure), that is calculated as the percentage of pixels which are an edge in the image, and the Fractal Dimension (FD measure) defined by Mandelbrot in [41], that is estimated by following the blanket method introduced by Peleg in [42].

The second group includes the measures obtained by applying statistics over matrices that collect information about the relationships between the gray level of each pixel and their neighbours. The measures of Haralick [29], that are based on the GLCM matrix, are placed in this group. In particular, 6 coarseness measures are obtained by applying the statistics contrast, correlation, entropy, local homogeneity, variance and uniformity over this matrix. This group also

Figure 2: Some examples of images with different degrees of fineness.

includes the measure defined by Amadasun in [30], the Short Run Emphasis (SRE measure) given by Galloway in [43], the Small Number Emphasis (SNE measure) defined by Sun *et al.* in [44], the Distribution of Gray Level Difference (DGD measure) proposed by Kim *et al.* in [45], and the measure defined by Weszka *et al.* in [46].

The third group is composed of two measures that are based on the Fourier power spectrum of the image. The first one is the measure used by Newsam in [47], computed as the average of power spectrum over ring-shaped regions centered at the origin, and the second one is the first moment of the power spectrum (FMPS measure), obtained by computing the mean value of Fourier power spectrum of the image [48].

However, according to the study performed in [38], some of the above measures have an unsuitable behavior. The measures of Newsam, FMPS, Entropy and uniformity are size dependent, i.e. the values given by these measures are affected by the window size. In addition, the Variance measure does not provide a representative information about the perception of fineness. Thus, these five measures are rejected and they will not be taken into account in the following, focusing our study on the other 12 measures, that are listed in the first column of Table 1. Besides the independence with the image size and the ability to provide information about the fineness perception, other interesting properties for texture analysis are also fulfilled by the proposed measures. As it is shown in [38], they are robust against changes in the image characteristic, like brightness and contrast, and they have a suitable behavior regarding the presence of noise in the image.

4 Assessment Collection

In this section, the way to obtain the set of values $\Gamma = \{v_1, \ldots, v_N\}$, that represents the presence degree of fineness perceived by humans in the images $I_i \in \mathcal{I}$, will be described. For this purpose, firstly the image set $\mathcal{I}$ will be selected (section 4.1). After that, a poll for getting assessments about the perception of fineness will be designed (section 4.2). Finally, for a given image, the assessments of the different subjects will be aggregated (section 4.3).

4.1 The texture image set

A set $\mathcal{I} = \{I_1, \ldots, I_N\}$ of $N = 80$ images representing examples of the fineness property has been selected. Figure 2 shows some images extracted from the set $\mathcal{I}$. Such set has been selected satisfying the following conditions:

- It covers the different presence degrees of fineness.
- The number of images for each presence degree is representative enough.
- Each image shows, as far as possible, just one presence degree of fineness.

Due to the third condition, each image can be viewed as "homogeneous" respect to the presence degree of fineness, i.e., if we select two random windows (with a dimension which does not "break" the original texture primitives and structure), the perceived fineness presence will be similar for each window (and also with respect to the original image). In other words, we can see each image $I_i \in \mathcal{I}$ as a set of lower dimension images (sub-images) with the same presence degree of the original one. This will be very useful for the fitting process, because we can have a larger number of fitting points without extending the number of images used in the poll.

4.2 The poll

Given the image set $\mathcal{I}$, the next step is to obtain assessments about the perception of fineness from a set of subjects. From now on, we will denote by $\Theta^i = [o_1^i, \ldots, o_L^i]$ the vector of assessments obtained from L subjects for the image I_i. We considered two alternatives to get Θ^i:

- To ask subjects about a presence degree between 0 and 1 for each image in the set.
- To ask subjects to assign images to classes, so that each class has associated a presence degree. In our proposal, an example image which represents the presence degree is associated to each class.

The first choice allows subjects to have more freedom to assess the presence degree of fineness. However, according to our own experience, it is very difficult for a subject to provide a value between 0 and 1 that represents the presence

degree of a certain texture concept (except in the case of both extremes: fulfillment of the concept -degree of 1- and unfulfillment of the concept -degree of 0). Thus, this alternative was discarded.

The above problem is solved by the second choice. The subject does not assess a value but classifies each image into a class, giving his opinion about the presence degree of fineness. One of the classes represents the presence degree of 1 of the fineness concept, i.e. a very fine texture. In our proposal, traditional examples used in the literature to define very fine textures has been considered for this class [49]. An example of this texture fineness is presented in the image shown in Figure 2(a). Another of the classes considered in the poll represents the presence degree of 0 of the fineness concept. In this case, again, traditional examples used in the literature to define very coarse textures has been considered for this class. Figure 2(i) shows an example of this presence degree of fineness. It should be noticed that textures coarser than this one will be also classified in this class, like the image shown in Figure 2(j). The rest of classes represent presence degrees of the fineness concept between 0 and 1, i.e. texture primitives scaled in size between the previous ones. In particular, nine classes have been considered in the pool. The first nine images shown in Figure 2 are the representative images for these classes. It should be noticed that these images are in decreasing order according to the presence degree of the fineness concept.

In our approach, 20 subjects have participated in the poll. As result, a vector of 20 assessments $\Theta^i = [o_1^i, \ldots, o_{20}^i]$ is obtained for each image $I_i \in \mathcal{I}$. The degree o_j^i associated to the assessment given by the subject S_j to the image I_i is computed as $o_j^i = (9-k) * 0.125$, where $k \in \{1, \ldots, 9\}$ is the index of the class to which the image is assigned by the subject.

4.3 Assessment aggregation

Our aim at this point is to obtain, for each image in the set $\mathcal{I}$, one assessment v_i that summarizes the assessments Θ^i given by the different subjects about the presence degree of fineness. To aggregate opinions we have used an OWA operator guided by a quantifier [50]. Concretely, the quantifier "the most" has been employed, which allows us to represent the opinion of the majority of the subjects. This quantifier is defined as

$$Q(r) = \begin{cases} 0 & \text{if } r < a, \\ \frac{r-a}{b-a} & \text{if } a \leq r \leq b, \\ 1 & \text{if } r > b \end{cases} \tag{2}$$

with $r \in [0, 1]$, $a = 0.3$ and $b = 0.8$. Once the quantifier Q has been chosen, the weighting vector of the OWA operator can be obtained following Yager [50] as $w_j = Q(j/L) - Q((j-1)/L), j = 1, 2, ..., L$. According to this, for each image $I_i \in \mathcal{I}$, the vector Θ^i obtained from L subjects will be aggregated into one assessment v^i as follows:

$$v_i = w_1 \hat{o}_1^i + w_2 \hat{o}_2^i + ... + w_L \hat{o}_L^i \tag{3}$$

where $[\hat{o}_1^i, \ldots, \hat{o}_L^i]$ is a vector obtained by ranking in nonincreasing order the values of the vector Θ^i.

5 Fitting the Membership Function

For a given subset of measures $\mathcal{F} \subseteq \mathbb{F}$, we aim to obtain the corresponding membership function $\mathcal{T}_\mathcal{F}$. In this paper, we propose to find a function that associates the values of the fineness measures with the human assessments about this property. As it was pointed out in section 4.1, thanks to the "homogeneity" in the presence degree of fineness, each image $I_i \in \mathcal{I}$ can be seen as a set of sub-images with the same fineness degree v_i of the original one. From now on, we will denote by $\mathcal{I}_\mathcal{W} = \{I_{i,w}, i = 1, \ldots, N; w = 1, \ldots, W\}$ the set of sub-images extracted from $\mathcal{I}$, where $I_{i,w}$ is the w-th sub-image of I_i and W is the number of sub-images considered for each image. According to this notation, let $\mathcal{I}_\mathcal{W}^{fit} \subset \mathcal{I}_\mathcal{W}$ and $\mathcal{I}_\mathcal{W}^{test} = \mathcal{I}_\mathcal{W} \backslash \mathcal{I}_\mathcal{W}^{fit}$ be two complementary subsets of $\mathcal{I}_\mathcal{W}$, that will be used for fitting the membership function and testing the obtained model, respectively. On the other hand, given a sub-image $I_{i,w}$, we will denote by $\mathbf{M}_\mathcal{F}^{i,w} = [m_1^{i,w}, \ldots, m_{K'}^{i,w}]$ the corresponding vector of measures, with $m_k^{i,w}$ being the result of applying the measure $F_k \in \mathcal{F}$ to $I_{i,w}$.

Thus, in order to estimate the membership function that associates the measure vectors ($\mathbf{M}_\mathcal{F}^{i,w}$) and the human assessments of fineness (v_i), we propose to fit a suitable function of the form given in Eq. (1) to the subset of points:

$$\Psi_\mathcal{F}^{fit} = \{(\mathbf{M}_\mathcal{F}^{i,w}, v_i); \forall I_{i,w} \in \mathcal{I}_\mathcal{W}^{fit}\} \tag{4}$$

In this paper, for each image $I_i \in \mathcal{I}$, $W = 200$ sub-images of size 32×32 have been considered[2], so $\mathcal{I}_\mathcal{W}$ is formed by 16000 sub-images. We propose to randomly select 75% of them for the fitting, so 12000 points are contained within $\Psi_\mathcal{F}^{fit}$.

The measure values can be affected by some factors, like brightness, contrast or noise, which typically causes outliers in the fitting points. For this reason, in our approach the membership function is calculated by means of a Robust Fitting of the multiset $\Psi_\mathcal{F}^{fit}$. In this modelling, the robust fitting based on M-estimators has been employed [51]. M-estimators are a generalization of the traditional maximum likelihood estimation, and, therefore, of the least squares fitting. If we consider a function $\mathcal{T}_F$ defined by D parameters $p_1, \ldots, p_D$, these parameters will be obtained as follows:

$$\underset{p_1,\ldots,p_D}{\operatorname{argmin}} \sum_{i=1}^{N} \rho\left(\mathbf{r}_w^i\right) \tag{5}$$

[2] As mentioned in Section 3, the measures used in this study are not size dependent. Therefore, the fineness models obtained by means of the fitting process do not depend on the window size. Sub-images smaller than 32×32 are not considered because they would break texture primitives.

Table 1: Fitting error and test error related to each measure, and graphical representation of the model with the lowest error.

Measure	Fitting error	Test error
Amadasun	0.1333	0.1695
Correlation	0.1401	0.1747
Abbadeni	0.1639	0.1947
FD	0.1776	0.2084
Tamura	0.1913	0.2070
ED	0.2009	0.2168
DGD	0.2031	0.2339
LH	0.2150	0.2336
Weszka	0.2157	0.2411
Contrast	0.2161	0.2475
SNE	0.2267	0.2418
SRE	0.2296	0.2455

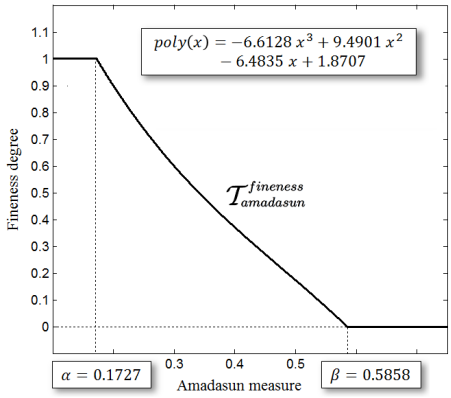

where $\mathbf{r}_w^i$ are the fitting residuals, and the function ρ, whose objective is to reduce the effect of outliers, gives the contribution of each residual in the model. In particular, in our approach we have taken one of the most commonly used functions in literature, that achieves a robust outlier rejection: the Tukey's biweight function [52].

For the fitting process, the number of measures K' within the set $\mathcal{F}$ should be taken into account. In this paper, we have focused our analysis on the cases of $K' = 1$ and $K' = 2$. The unidimensional case ($K' = 1$) will allow us to study each measure separately, comparing its goodness respect to the others (preliminary studies were presented in our previous work [39], that are summarized in section 5.1). In the bidimensional case ($K' = 2$), pairs of measures will be taken in order to improve the unidimensional models (section 5.2). For higher dimensions ($K' \geq 3$), the fitting based on M-estimators is too complex, so new methods for finding $\mathcal{T}_\mathcal{F}$ need to be considered (for example, some kind of heuristic approaches). These cases will be considered in future works.

5.1 Unidimensional case

In the case of $K' = 1$ each measure $F_k \in \mathbb{F}$ is studied separately [39]. To define $\mathcal{T}_\mathcal{F}$ the following considerations will be taken into account:

- The values $\mathcal{T}_\mathcal{F}(x) = 0$ and $\mathcal{T}_\mathcal{F}(x) = 1$ should be achieved.
- $\mathcal{T}_\mathcal{F}$ should be a monotonic function.

Regarding the above properties, we propose to define $\mathcal{T}_\mathcal{F}$ as a function

$$\mathcal{T}_\mathcal{F} : \mathbb{R} \rightarrow [0, 1] \tag{6}$$

of the form[3]

$$\mathcal{T}_{\mathcal{F}}(x; a_n \dots a_0, \alpha, \beta) = \begin{cases} 1 & x < \alpha, \\ poly(x; a_n \dots a_0) & \alpha \leq x \leq \beta, \\ 0 & x > \beta \end{cases} \tag{7}$$

with $poly(x; a_n \dots a_0)$ being a polynomial function

$$poly(x; a_n \dots a_0) = a_n x^n + \dots + a_1 x^1 + a_0 \tag{8}$$

In our proposal [39], the parameters $a_n \dots a_0$, α and β of the function $\mathcal{T}_{\mathcal{F}}$ are calculated by carrying out a robust fitting on $\Psi_{\mathcal{F}}^{fit}$, with the constraint to obtain a strictly monotonic function between α and β. For the polynomial function, the cases of $n = 1, 2, 3, 4$ (i.e. linear, quadratic, cubic and quartic functions) have been considered.

The second column of Table 1 shows for each measure $F_k \in \mathbb{F}$ the least fitting error obtained [39]. Note that this value can be viewed as the goodness of each measure to represent the perception of fineness. Table 1 has been ranked in increasing order of these fitting errors. In all the cases, the least error has been obtained for a polynomial function of order $n = 3$ (the use of higher order functions does not provide better fits).

In addition, the test error for each measure has been calculated by using the subset of points $\Psi_{\mathcal{F}}^{test}$ and it is shown in the third column of Table 1. In our approach, this error is calculated as the mean absolute difference between the values v_i and the degrees obtained by applying the function $\mathcal{T}_{\mathcal{F}}$ to the values $\mathbf{M}_{\mathcal{F}}^{i,w}$, for all the points $(\mathbf{M}_{\mathcal{F}}^{i,w}, v_i) \in \Psi_{\mathcal{F}}^{test}$, i.e.

$$E^{test} = \frac{\sum_{(\mathbf{M}_{\mathcal{F}}^{i,w}, v_i) \in \Psi_{\mathcal{F}}^{test}} \left| \mathcal{T}_{\mathcal{F}}(\mathbf{M}_{\mathcal{F}}^{i,w}) - v_i \right|}{card(\Psi_{\mathcal{F}}^{test})} \tag{9}$$

with $card(\Psi_{\mathcal{F}}^{test})$ being the cardinality of $\Psi_{\mathcal{F}}^{test}$.

The parameters of the membership function with the lowest error, corresponding to the measure of Amadasun, as well as its graphical representation, are shown on the right of Table 1 [39].

5.2 Bidimensional case

In the case of $K' = 2$, the membership function $\mathcal{T}_{\mathcal{F}}$ will have two variables, corresponding to the pair of measures used as reference set. To define this function, the following considerations will be taken into account:

- The values $\mathcal{T}_{\mathcal{F}}(\mathbf{x}) = 0$ and $\mathcal{T}_{\mathcal{F}}(\mathbf{x}) = 1$ should be achieved from a certain value.

[3] Note that this function is defined for measures that decrease according to the perception of fineness. For those that increase, the function needs to be changed appropriately, i.e. it takes the value 0 for $x < \beta$, it takes the value 1 for $x > \alpha$, and the polynomial function is computed for $\beta \leq x \leq \alpha$.

Table 2: Fitting error and test error related to each pair of measures.

Measure x	Measure y	Fitting error	Test error
FD	Amadasun	0.1053	0.1574
Amadasun	Correlation	0.1306	0.1660
Correlation	FD	0.1180	0.1733
Abbadeni	Amadasun	0.1313	0.1673
Correlation	ED	0.1361	0.1741
Correlation	Abbadeni	0.1400	0.1724
Tamura	Amadasun	0.1207	0.1666
Abbadeni	Tamura	0.1404	0.1833
Correlation	Tamura	0.1368	0.1740
Amadasun	ED	0.1330	0.1688
FD	Tamura	0.1486	0.1980
Abbadeni	ED	0.1521	0.1925
Abbadeni	FD	0.1510	0.1861
Tamura	ED	0.1738	0.1939
ED	FD	0.1782	0.1944

- $\mathcal{T}_{\mathcal{F}}$ should be a "monotonic" function in the sense that its gradient must satisfy the following condition:

$$\|\nabla \mathcal{T}_{\mathcal{F}}(\mathbf{x})\| \neq 0 \quad \forall \mathbf{x} \ / \ 0 < \mathcal{T}_{\mathcal{F}}(\mathbf{x}) < 1 \tag{10}$$

Regarding the above properties, we propose to define $\mathcal{T}_{\mathcal{F}}$ as a function

$$\mathcal{T}_{\mathcal{F}} : \mathbb{R}^2 \rightarrow [0,1] \tag{11}$$

of the form

$$\begin{aligned} &\mathcal{T}_{\mathcal{F}}(x,y;a_{(n!+n)} \dots a_0) = \mathcal{T}_{\mathcal{F}}(x,y;coef) = \\ &= \begin{cases} 1 & poly2(x,y;coef) > 1, \\ poly2(x,y;coef) & 0 < poly2(x,y;coef) < 1, \\ 0 & poly2(x,y;coef) < 0 \end{cases} \end{aligned} \tag{12}$$

with $poly2(x,y;coef)$ being a polynomial function of two variables

$$poly2(x,y;a_{(n!+n)} \dots a_0) = \sum_{i=0}^{n} \sum_{j=0}^{i} a_{(i!+j)} x^j y^{i-j} \tag{13}$$

As in the unidimensional case, the parameters $a_{(n!+n)} \dots a_0$ of the function $\mathcal{T}_{\mathcal{F}}$ will be calculated by carrying out a robust fitting on $\Psi_{\mathcal{F}}^{fit}$. Furthermore, the cases of $n = 1, 2, 3, 4$ have been considered for the polynomial function.

Table 2 shows the least fitting error and the test error obtained for each pair of measures. Only the combination of the first six measures in Table 1 are shown, and, in all the cases, the least error has been obtained for a polynomial

Parameters for $\{FD, Amadasun\}$	
a_9	0.4175
a_8	-38.064
a_7	0.0000
a_6	-0.6475
a_5	-4.5174
a_4	51.149
a_3	1.5584
a_2	15.194
a_1	-27.351
a_0	-12.156

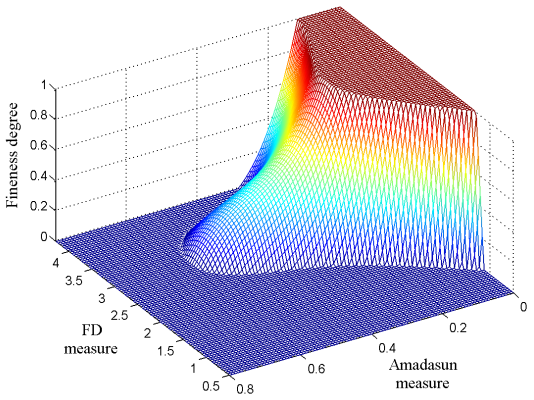

Figure 3: Parameters and graphical representation of the membership function $\mathcal{T}_{\mathcal{F}}$ corresponding to the pair of measures $\mathcal{F} = \{FD, Amadasun\}$.

function of order $n = 3$. It can be noticed that the combination of both measures allows us to reduce the error obtained by applying each one separately. This implies that the use of bidimensional functions provides models that fit more closely to the perception of fineness than in the unidimensional case. In our experiments, the pair of measures $\mathcal{F} = \{FD, Amadasun\}$ gives the best results. The parameters corresponding to this membership function, as well as its graphical representation, are shown in Figure 3.

6 Results

In this section, the goodness of the fuzzy models proposed for texture modelling will be analyzed. First, in section 6.1, we will compare them with the state of the art in the modelling of the fineness texture property. Then, in section 6.2 we will show the results obtained by applying these models to several experiments with images. In particular, the fuzzy sets with least fitting error and least test error for the unidimensional case and the bidimensional case (corresponding to the measure of Amadasun and the pair of measures $\mathcal{F} = \{FD, Amadasun\}$, respectively) will be used.

6.1 Comparison with the state of the art

At this point, the aim is to compare the fuzzy sets obtained in section 5 with the state of the art in the modelling of visual texture properties. As has been commented throughout this paper, the proposed fuzzy models allow to represent the presence degree of the fineness texture property, and we have verified by means of goodness measures (fitting errors and test errors) that the obtained degrees match with the human perception of this property. However, as we have

shown in section 1, there is no other fuzzy approach in the literature with the ability of providing this type of information. Nevertheless, most of the existing crisp measures (shown in section 3) allow to represent the fineness property in the sense that the greater the value given by the measure, the greater (lower) the presence of this property. With this in mind, and in order to compare the different approaches, we will study whether the increase in the value of a measure is always produced by the increase (or decrease) in the fineness presence.

In particular, two comparative studies will be performed using the subset of images $\mathcal{I}_{\mathcal{W}}^{test}$. In the first one, we will study the correlation between the order given by the measure values computed from the images in $\mathcal{I}_{\mathcal{W}}^{test}$ and the order of these images according to the poll[4]. To do this, we propose to use the Kendall rank correlation coefficient [53] and the Spearman rank correlation coefficient [54], that are widely used in this type of problems. The Kendall coefficient is defined as:

$$\tau = \frac{n_c - n_d}{n(n-1)/2} \tag{14}$$

with n being the number of ranked elements, and where n_c and n_d are the number of concordant and discordant pairs comparing both rankings, as it is shown in [53]. The Spearman coefficient is defined as:

$$\rho = \frac{\sum_i (x_i - \bar{x})(y_i - \bar{y})}{\sqrt{\sum_i (x_i - \bar{x})^2 \sum_i (y_i - \bar{y})^2}} \tag{15}$$

with x_i and y_i being the rank of each pair of elements in its corresponding ranking, and with $\bar{x}$ and $\bar{y}$ being the mean of the values in each ranking. In both cases, a higher coefficient indicates a better correlation between the ranking of the measure values and the ranking of the human assessments about the presence of the property.

In the second comparative study, the significance of each model will be analyzed. In this case, we study whether the values given by the model for textures with different fineness presence are significantly different compared to the values obtained from textures with a similar presence. For this purpose, the F-statistic [55] will be computed from the R^p classes in which the images in $\mathcal{I}_{\mathcal{W}}^{test}$ have been grouped in the poll. This statistic compares the between-group variation of the values with their within-group variation as follows:

$$F = \frac{\sum_{i=1}^{k} n_i (\bar{x}_i - \bar{x})^2 / (k-1)}{\sum_{i=1}^{k} \sum_{j=1}^{n} (x_{ij} - \bar{x}_i)^2 / (N-k)} \tag{16}$$

where k is the total number of groups, n_i is the number of elements in the i-th group, N is the total numer of elements, x_{ij} represents the j-th element in group i, $\bar{x}_i$ is the mean in group i, and $\bar{x}$ is the mean of all the elements. A higher F-statistic means that the model has more significance, i.e. it allows to distinguish more clearly different presence degrees of fineness.

[4]Note that in this case we are not interested in the specific assessment associated to each image, but in the ranking of these values.

In these two studies, we will compare the fuzzy models proposed in this paper for the unidimensional and bidimensional cases (the models with the highest goodness according to fitting and test errors) with the state of the art in the modelling of texture properties, consisting of all the crisp measures shown in section 3, as well as the fuzzy approaches commented in section 1. Note that these fuzzy approaches are based on partitions, so they do not provide a presence degree of fineness, but a set of linguistic labels (and their corresponding membership degrees) to describe this property. Thus, this information cannot be used directly in the proposed comparative studies. However, from a semantical point of view, this information also provides a presence estimation of the fineness property, although it is represented in a different mathematical format. In this sense, it can be ranked on the basis of the linguistic labels, that are semantically ordered according to the presence of fineness. This way, given an image from the set $\mathcal{I}_{\mathcal{W}}^{test}$, we associate it to the linguistic label with the highest membership degree, obtaining a ranking that can be used in the comparative studies. As has been commented in section 1, the majority of the fuzzy approaches in the literature [26, 36, 28, 56, 37] propose a fuzzy partition with five linguistic terms defined on the domain of the fineness measure defined by Tamura. According to these approaches, we have generated the fuzzy partitions through an unsupervised fuzzy clustering algorithm on the basis of the measure values obtained from the subset of images $\mathcal{I}_{\mathcal{W}}^{fit}$. As all these approaches propose a similar solution, we have included the item *"FuzzyP"* in the comparative studies, that represents all them.

Tables 3(a) and 3(b) show the results obtained in these two studies, respectively. The first table is ranked in decreasing order of the Spearman rank correlation coefficient, while the second one is ranked in decreasing order of the F-statistic. As can be seen, the best approach in all the comparative studies is the fuzzy model proposed in this paper for the bidimensional case, followed by the fuzzy model corresponding to the unidimensional case. Note that the values of both correlation coefficients in Table 3(a) are relatively low. This is due only to the fact that nine different classes of fineness have been considered in the poll and there is much overlap between them, which is also reflected in the corresponding study of significance (Table 3(b)).

Therefore, although the full potential of our approach is not being used in these comparative studies, the obtained results show that, in the experiment performed in this paper, our approach already improves the state of the art. In order to appreciate the ability of our fuzzy models to represent the presence degree of the fineness property, which is not reflected in these comparative studies, the results obtained by applying these models to experiments with different images will be shown in next section.

6.2 Experiments with images

In this section, four experiments using both the unidimensional and bidimensional models are shown. In the first one, which was also employed to illustrate our preliminary studies in [39], the unidimensional model is applied; in the sec-

Table 3: Comparative study of rank correlation by means of Spearman and Kendall coefficients (a), and comparative study of significance by means of the F-statistic (b).

Fineness model	Spearman coefficient	Kendall coefficient
Chamorro2D	0.7346	0.5913
Chamorro1D	0.7303	0.5705
Amadasun	0.7299	0.5660
Correlation	0.7289	0.5610
Abbadeni	0.6981	0.5293
ED	0.6407	0.4744
FD	0.6163	0.4545
Tamura	0.6118	0.4567
FuzzyP	0.5983	0.4781
DGD	0.5629	0.4197
LH	0.5624	0.4132
Weszka	0.5436	0.4039
SRE	0.5413	0.3984
Contrast	0.4923	0.3674
SNE	0.4857	0.3555

(a)

Fineness model	Significance (F-statistic)
Chamorro2D	174.3169
Chamorro1D	168.7424
Correlation	155.9657
Tamura	125.0183
Amadasun	118.1959
FuzzyP	115.7747
FD	114.4741
ED	110.3823
DGD	70.7770
LH	69.6480
Weszka	65.5035
SNE	66.7699
SRE	53.0102
Abbadeni	42.4382
Contrast	34.0349

(b)

ond one, both models are used in order to compare the obtained results; and in the last two experiments only the bidimensional model is applied.

For the first experiment, we have considered Figure 4(a), corresponding to a mosaic made by several texture images, each one with a different increasing perception degree of fineness. These images are part of the set $\mathcal{I}$ used in the poll, so human assessments about fineness presence are available in order to compare them with the obtained results.

Figure 4(b) shows an ideal mapping from the original mosaic image to its fineness values, where all pixels corresponding to the same texture image have been mapped using the human assessment associated to that image[5]. These assessments (between 0 and 1) have been mapped into a gray level from 0 to 255, so that a white pixel in the mapping indicates maximum perception of fineness, while a black one indicates no perception of fineness (maximum perception of coarseness).

Figure 4(c) shows a mapping from the original image to its fineness values obtained by applying the proposed unidimensional model. For each pixel in the original image, a centered window of size 32×32 has been analyzed and its

[5]Actually, note that an ideal mapping would not be exactly as shown in the figure, because pixels near the boundary of different textures would have an intermediate fineness value of both textures.

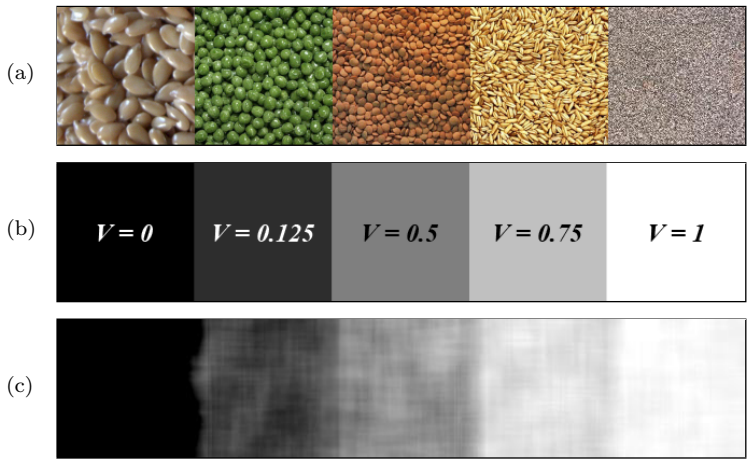

Figure 4: Result for a mosaic image (a), comparing the human assessments about the presence degree of fineness (b) and the membership degrees obtained by applying the proposed unidimensional model (c).

fineness membership degree has been calculated. This degree has been mapped into a gray level from 0 to 255. It can be noticed that our model captures the evolution of the perception degrees of fineness, and the obtained mapping, that represents the estimated presence degree of this property, can be directly interpreted by humans.

In this first experiment, the use of the unidimensional fineness model has already given good results. In fact, if the proposed bidimensional fineness model is applied, very similar mappings are obtained. However, with others textures, as the ones shown in the following experiments, the unidimensional model does not have a good performance, so the bidimensional model is needed to improve the obtained results. Let's consider Figure 5(a) corresponding to a mosaic made by several texture images, each one with a different increasing perception degree of fineness. As in the previous experiment, these images are part of the set $\mathcal{I}$ used in the poll, so human assessments about fineness presence are available in order to compare with the obtained results. Figure 5(b) shows an ideal mapping from the original mosaic image to its fineness values, where all pixels within the same texture image have been mapped using the corresponding human assessment. Moreover, the histogram associated to this mapping image has also been represented in Figure 5(b), and we can see the four peaks corresponding to the four different fineness degrees in the image.

Figure 5(c) shows a mapping from the original image to its fineness values using the bidimensional model corresponding to the pair of measures $\mathcal{F} = \{FD, Amadasun\}$, while figure 5(d) and 5(e) show a mapping using the unidimensional model of each measure separately (Amadasun and FD, respectively). It can be noticed that in this case the unidimensional models are not able to

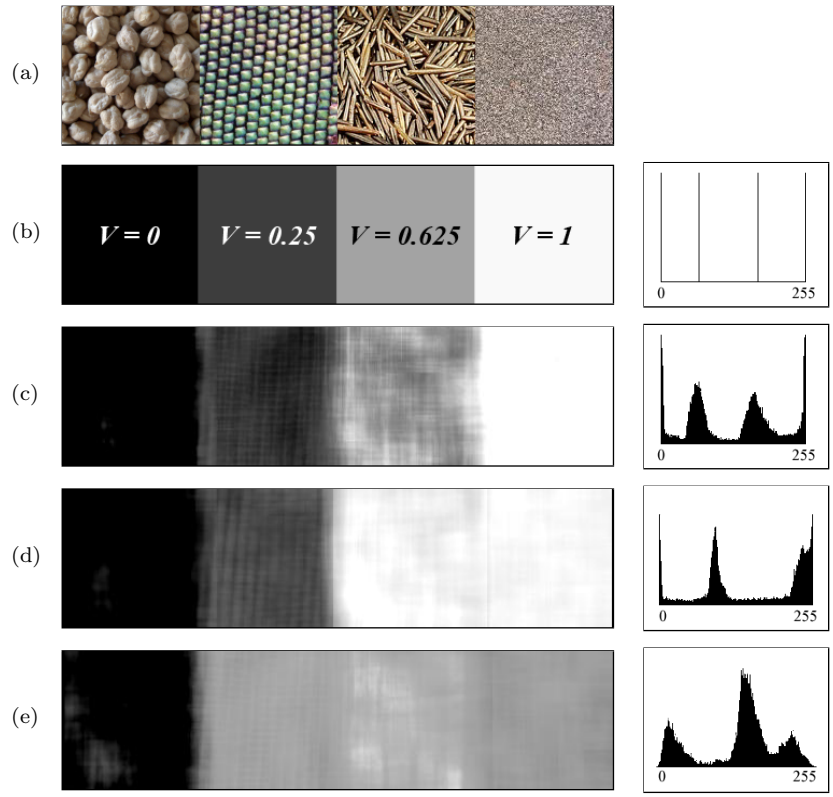

Figure 5: Result for a mosaic image (a), comparing the human assessments about the presence degree of fineness (b) with the membership degrees obtained by applying the bidimensional model for the measures $\mathcal{F} = \{FD, Amadasun\}$ (c) and the unidimensional models for each measure separately (Amadasun (d) and FD (e)), as well as the histograms of the corresponding mappings.

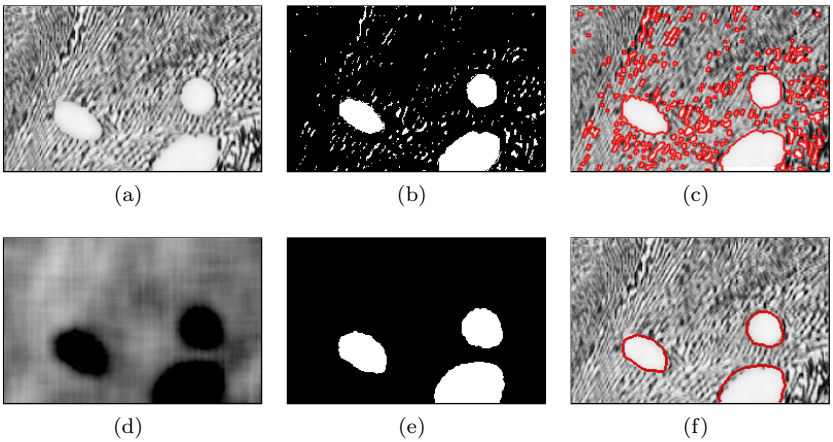

Figure 6: Pattern recognition. (a) Original image. (b) Binary image obtained by thresholding the original one. (c) Region outlines of b superimposed on the original image. (d) Fineness membership degrees from the original image using the proposed model. (e) Binary image obtained by thresholding d. (f) Region outlines of e superimposed on the original image.

capture the evolution of the perception degrees of fineness, while the bidimensional model can do it. Moreover, comparing the histogram of these mappings, we can clearly see four different peaks in the histogram corresponding to the bidimensional model, as it captures the four different fineness degrees in the image, while in the other two histograms only three peaks can be identified. Therefore, we can state that the bidimensional model represents more faithfully the fineness perception, giving results that match what a human would expect.

In the third experiment, the proposed bidimensional fineness model has been employed for pattern recognition. In this case, the microscopy image shown in Figure 6(a), corresponding to the microstructure of a metal sample, has been used. The lamellae indicates islands of eutectic, which are to be separated from the uniform light regions. The brightness values in regions of the original image are not distinct, so texture information is needed for extracting the uniform areas. This fact is showed in figures 6(b) and 6(c), where a thresholding on the original image is displayed (homogeneous regions cannot be separated from the textured ones as they "share" brightness values).

Figure 6(d) shows a mapping from the original image to its fineness membership degrees. It can be noticed that uniform regions correspond to areas with low degrees of fineness (i.e., high coarseness), so if only the pixels with fineness degree lower than 0.1 are selected (which is equivalent to a coarseness degree upper than 0.9, i.e. an α-cut of the coarseness fuzzy set with $\alpha = 0.9$), the uniform light regions emerge with ease, as it is shown in figures 6(e) and 6(f).

The fourth experiment, that is presented in Figure 7, shows another example

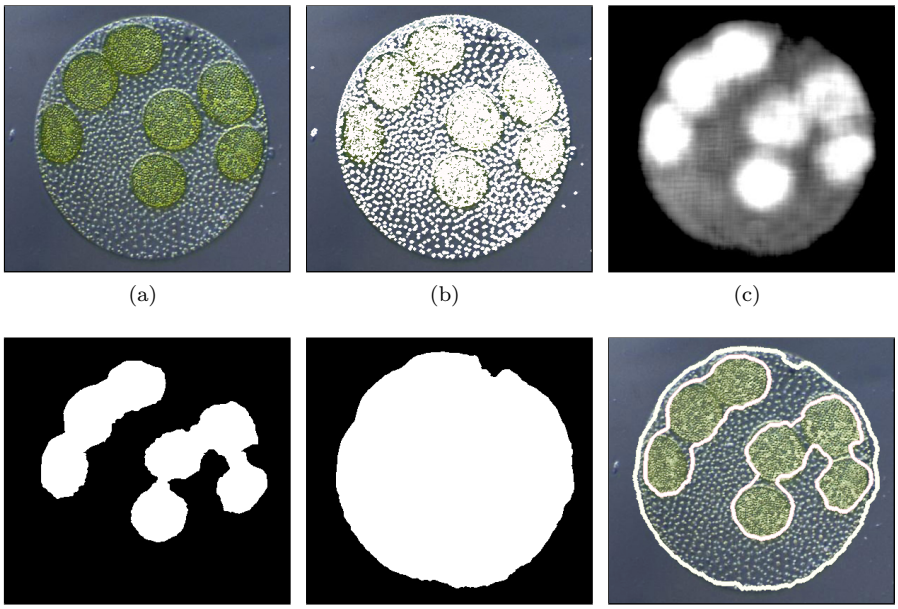

Figure 7: Pattern recognition. (a) Original image. (b) Region outlines obtained by thresholding the original image. (c) Fineness membership degrees from the original image using the proposed bidimensional model. (d)(e) Binary images obtained by applying two different thresholds to c. (f) Region outlines of d and e superimposed on the original image.

where the proposed bidimensional fineness model has been employed for pattern recognition. Figure 7(a) shows the natural image used in this example, that corresponds to a microscopic image of a volvox (a colony of greencells). In this case, we want to separate the main colony from the background and the daughter colonies from the mother colony. As in the previous example, this cannot be done by thresholding on the original image, as it is shown in Figure 7(b), so texture information is needed. Figure 7(c) shows a mapping from the original image to its fineness membership degrees. Three different degrees of fineness can be clearly identified: a very fine texture (pixels in white) corresponding to the daughter colonies of greencells that are inside the main colony, an intermediate coarseness texture (pixels with an intermediate grey level) corresponding to the main colony and a very coarse texture (pixels in black) corresponding to the background. Thus, daughter colonies can be obtained by selecting the pixels with fineness degree higher than 0.9., i.e. an α-cut of the fuzzy set with $\alpha = 0.9$, as it is shown in Figure 7(d). On the other hand, the main colony can be separated from the uniform background by selecting the pixels with fineness degree lower than 0.1, as it is shown in Figure 7(e). Finally, the region outlines

of figures 7(d) and 7(e) superimposed on the original image are shown in Figure 7(f).

7 Conclusions and Future Works

In this paper, a perception-based fuzzy approach for texture modelling has been proposed. For this modelling, fuzzy sets defined on the domain of representative fineness measures have been employed, associating the concept of texture with the presence of the fineness property. In our approach, subsets of fineness measures have been used as reference set, allowing us to combine the ability of different measures to capture the presence of fineness. In order to define the fuzzy sets, parametric functions have been employed, where the corresponding parameters have been calculated by taking into account the relationship between the computational measures and the human perception of fineness. This way, the shape of the membership function has been adjusted to represent this relationship, and the obtained membership degrees match what a human would expect, as has been shown in the experiments of section 6. Moreover, the use of a unique fuzzy set to model the fineness concept as a whole has allowed its application to pattern recognition problems (e.g. the examples shown in figures 6 and 7).

In addition, our approach has been also employed to analyze the combination of fineness measures in order to identify the most appropriate pair for representing the fineness property. In the proposed modelling, some of the most representative measures in the literature have been employed, analyzing their ability to represent the perception of fineness. First, a ranking of individual measures has been obtained, that is shown in Table 1. This ranking allows us to analyze each measure separately, identifying the most appropriate one in this case, that is the fineness measure of Amadasun. Second, a ranking of pairs of measures has been achieved, which is shown in Table 2. Comparing both rankings, we have verified that the combination of measures improves the fineness characterization. Therefore, we can state that the bidimensional model proposed in this paper represents more faithfully the fineness perception, giving results that match what a human would expect. Moreover, according to the second ranking, we have concluded that the most suitable combination of measures to represent the fineness property corresponds to the pair $\mathcal{F} = \{FD, Amadasun\}$.

Regarding to the future work, as it has been commented in section 5, the fitting based on M-estimators is too complex for higher dimensions ($K \geq 3$). This complexity must be understood in the sense that the cost functions used in M-estimators are non-convex. This implies that the optimization problem may have many local optimal solutions, so a good initialization is needed, especially for high-dimensional problems. In our approach, suitable initial parameters can be found for the unidimensional and bidimensional cases by using non-robust fitting methods, but this is a non-trivial problem for higher dimensional models. Therefore, new methods for finding $\mathcal{T}_{\mathcal{F}}$ will be considered in future works (for example, some kind of heuristic approaches).

In addition, as it was pointed out, the fuzzy sets proposed in this paper have been obtained by using the assessments given by a group of subjects in the polls, so they are representing the average perception of fineness. Thus, these fuzzy sets can be considered as the default models for the fineness property, because they can be used if additional information is not available (user's profile, context, etc.). However, a particular user may have a different perception of fineness, and, moreover, the image context may influence the global perception. In order to take into account these considerations, an approach that allows us to adapt the default models to each particular case is needed. In this sense, we are working on a methodology to automatically adapt the membership function associated to each fuzzy set according to the information given by an user to represent his particular perception, or the information about the context extracted from the textures present in the image.

Acknowledgements

This work has been partially supported by the Spanish Government under the project TIN2014-58227 *"Descripción linguística de información visual mediante técnicas de minería de datos y computación flexible"*. We also would like to thank Dr. Daniel Sánchez for his valuable assistance in the field of fuzzy logic, as well as Elena Galán-Perales for her contribution in the human assessment collection.

References

[1] J. C. Russ, The Image Processing Handbook, 3rd Edition, CRC Press and IEEE Press, 1999.

[2] M. Tuceryan, A. K. Jain, The Handbook of Pattern Recognition and Computer Vision, 2nd Edition, World Scientific Publishing Co., 1998, Ch. Texture Analysis, pp. 207–248.

[3] A. R. Rao, G. L. Lohse, Identifying high level features of texture perception, Graphical Models and Image Processing 55 (3) (1993) 218–233.

[4] H. Tamura, S. Mori, T. Yamawaki, Textural features corresponding to visual perception, IEEE Transactions on Systems, Man and Cybernetics 8 (1978) 460–473.

[5] J. Han, K. K. Ma, Rotation-invariant and scale-invariant Gabor features for texture image retrieval, Image and Vision Computing 25 (9) (2007) 1474–1481.

[6] D. Zhang, A. Wong, M. Indrawan, G. Lu, Content-based image retrieval using Gabor texture features, in: Proceedings of the IEEE Pacific-Rim Conference on Multimedia, Sydney, Australia, 2000, pp. 392–395.

[7] X. Guang-mei, H. Wen, Z. Hai-ying, B. Hong, A new metric algorithm of image textural coarseness, in: Proceedings of the 2010 International Conference on Computer Application and System Modeling, Vol. 11, 2010, pp. 544–548.

[8] X. Xie, A review of recent advances in surface defect detection using texture analysis techniques, Electronic Letters on Computer Vision and Image Analysis 7 (3).

[9] S. Arivazhagan, L. Ganesan, Texture classification using wavelet transform, Pattern Recognition Letters 24 (9-10) (2003) 1513–1521.

[10] P. S. Hiremath, S. Shivashankar, Wavelet based features for texture classification, ICGST International Journal on Graphics, Vision and Image Processing 6 (3) (2006) 55–58.

[11] W. Y. Ma, B. S. Manjunath, A comparison of wavelet transform features for texture image annotation, in: Proceedings of the IEEE International Conference on Image Processing, Vol. 2, Washington, D.C., USA, 1995, pp. 256–259.

[12] M. Li, R. C. Staunton, Optimum Gabor filter design and local binary patterns for texture segmentation, Pattern Recognition Letters 29 (5) (2008) 664–672.

[13] G. Scarpa, R. Gaetano, M. Haindl, J. Zerubia, Hierarchical multiple Markov chain model for unsupervised texture segmentation, IEEE Transactions on Image Processing 18 (8) (2009) 1830–1843.

[14] F. Lehmann, Turbo segmentation of textured images, IEEE Transactions on Pattern Analysis and Machine Intelligence 33 (1) (2011) 16–29.

[15] S. Arivazhagan, L. Ganesan, S. P. Priyal, Texture classification using Gabor wavelets based rotation invariant features, Pattern Recognition Letters 27 (16) (2006) 1976–1982.

[16] Z. Guo, L. Zhang, D. Zhang, Rotation invariant texture classification using LBP variance (LBPV) with global matching, Pattern Recognition 43 (3) (2010) 706–719.

[17] M. Pietikäinen, A. Hadid, G. Zhao, T. Ahonen, Texture classification and segmentation, in: Computer Vision Using Local Binary Patterns, Vol. 40 of Computational Imaging and Vision, Springer London, 2011, pp. 69–79.

[18] M. Kokare, P. K. Biswas, B. N. Chatterji, Texture image retrieval using rotated wavelet filters, Pattern Recognition Letters 28 (10) (2007) 1240–1249.

[19] J. Yue, Z. Li, L. Liu, Z. Fu, Content-based image retrieval using color and texture fused features, Mathematical and Computer Modelling 54 (3-4) (2011) 1121 – 1127.

[20] J. Portilla, E. P. Simoncelli, A parametric texture model based on joint statistics of complex wavelet coefficients, International Journal of Computer Vision 40 (2000) 49–71.

[21] G. Xu, Y. Hong, A fast texture synthesis method based on cooccurrence matrix analysis, in: Proceedings of the 2nd IEEE International Conference on Computer Science and Information Technology (ICCSIT), 2009, pp. 536–540.

[22] A. Zalesny, L. V. Gool, A compact model for viewpoint dependent texture synthesis, in: Proceedings of the 2nd European Workshop on 3D Structure from Multiple Images of Large-Scale Environments (SMILE), Vol. 2018 of Lecture Notes in Computer Science, Springer, 2001, pp. 124–143.

[23] S. Battiato, G. Gallo, S. Nicotra, Perceptive visual texture classification and retrieval, in: Proceedings of the 12th International Conference on Image Analysis and Processing, Washington, DC, USA, 2003, pp. 524–529.

[24] B. S. Manjunath, Introduction to MPEG-7, Multimedia Content Description Interface, John Wiley and Sons, Ltd., 2002.

[25] M. Nirmala, K. Karthikeyan, S. Appalabatla, R. A. Ahmed, Image interpretation based on similarity measures of visual content descriptors. An insight, International Journal of Computer Science and Emerging Technologies 2 (2) (2011) 242–248.

[26] H. Aboulmagd, N. El-Gayar, H. Onsi, A new approach in content-based image retrieval using fuzzy, Telecommunication Systems 40 (1) (2009) 55–66.

[27] M. Flicker, H. Sawhney, W. Niblack, J. Ashley, Q. Huang, B. Dom, M. Gorkani, J. Hafner, D. Lee, D. Petkovic, D. Steele, P. Yanker, Query by image and video content: the QBIC system, IEEE Computer 28 (9) (1995) 23–32.

[28] H. C. Lin, C. Y. Chiu, S. N. Yang, Finding textures by textual descriptions, visual examples, and relevance feedbacks, Pattern Recognition Letters 24 (14) (2003) 2255–2267.

[29] R. M. Haralick, Statistical and structural approaches to texture, Proceedings IEEE 67 (5) (1979) 786–804.

[30] M. Amadasun, R. King, Textural features corresponding to textural properties, IEEE Transactions on Systems, Man and Cybernetics 19 (5) (1989) 1264–1274.

[31] N. Abbadeni, N. Ziou, D. S. Wang, Autocovariance-based perceptual textural features corresponding to human visual perception, in: Proceedings of the 15th International Conference on Pattern Recognition, Vol. 3, Barcelona, Spain, 2000, pp. 901–904.

[32] X. Huang, Automatic video text detection and localization based on coarseness texture, in: Proceedings of the Fifth International Conference on Intelligent Computation Technology and Automation, 2012, pp. 398–401.

[33] M. Nachtegael, E. Kerre, S. Damas, D. V. der Weken, Special issue on recent advances in soft computing in image processing, International Journal of Approximate Reasoning 50 (1) (2009) 1–2.

[34] C. Solana-Cipres, G. Fernandez-Escribano, L. Rodriguez-Benitez, J. Moreno-Garcia, L. Jimenez-Linares, Real-time moving object segmentation in h.264 compressed domain based on approximate reasoning, International Journal of Approximate Reasoning 51 (1) (2009) 99 – 114.

[35] C. Y. Chiu, H. C. Lin, S. N. Yang, A fuzzy logic CBIR system, in: Proceedings of the 12th IEEE International Conference on Fuzzy Systems, Vol. 2, St Louis, MO, USA, 2003, pp. 1171–1176.

[36] S. Kulkarni, B. Verma, Fuzzy logic based texture queries for CBIR, in: Proceedings of the 5th International Conference on Computational Intelligence and Multimedia Applications, Xi'an, China, 2003, pp. 223–228.

[37] B. Verma, S. Kulkarni, A fuzzy-neural approach for interpretation and fusion of colour and texture features for CBIR systems, Applied Soft Computing 5 (1) (2004) 119–130.

[38] J. Chamorro-Martínez, P. Martínez-Jiménez, A comparative study of texture coarseness measures, in: Proceedings of the 16th IEEE International Conference on Image Processing, Cairo, Egypt, 2009, pp. 1337–1340.

[39] J. Chamorro-Martinez., P. M. Martinez-Jimenez, J. M. Soto-Hidalgo, B. Prados-Suarez, Perception-based fuzzy sets for visual texture modelling, Soft Computing 18 (12) (2014) 2485–2499.

[40] S. W. Zucker, D. Terzopoulos, Finding structure in co-occurrence matrices for texture analysis, Computer Graphics and Image Processing 12 (3) (1980) 286 – 308.

[41] B. B. Mandelbrot, The fractal geometry of nature, Freeman, San Francisco, 1982.

[42] S. Peleg, J. Naor, R. Hartley, D. Avnir, Multiple resolution texture analysis and classification, IEEE Transactions on Pattern Analysis and Machine Intelligence 6 (4) (1984) 518–523.

[43] M. M. Galloway, Texture analysis using gray level run lengths, Computer Graphics and Image Processing 4 (1975) 172–179.

[44] C. Sun, W. G. Wee, Neighboring gray level dependence matrix for texture classification, Computer Vision, Graphics and Image Processing 23 (1983) 341–352.

[45] S. I. Kim, K. C. Choi, D. S. Lee, Texture classification using run difference matrix, in: Proceedings of the 1991 IEEE Ultrasonics Symposium, Vol. 2, Orlando, FL, USA, 1991, pp. 1097–1100.

[46] J. S. Weszka, C. R. Dyer, A. Rosenfeld, A comparative study of texture measures for terrain classification, IEEE Transactions on Systems, Man, and Cybernetics 6 (4) (1976) 269–285.

[47] S. D. Newsam, C. Kammath, Retrieval using texture features in high resolution multi-spectral satellite imagery, in: Proceedings of Data Mining and Knowledge Discovery: Theory, Tools, and Technology VI, Vol. 5433, Orlando, FL, USA, 2004, pp. 21–32.

[48] H. Yoshida, D. D. Casalino, B. Keserci, A. Coskun, O. Ozturk, A. Savranlar, Wavelet-packet-based texture analysis for differentiation between benign and malignant liver tumours in ultrasound images, Physics in Medicine and Biology 48 (2003) 3735–3753.

[49] P. Brodatz, Textures: a photographic album for artists and designers, Dover Publishing Co., 1966.

[50] R. R. Yager, On ordered weighted averaging aggregation operators in multicriteria decisionmaking, IEEE Transactions on Systems, Man and Cybernetics 18 (1) (1988) 183–190.

[51] P. J. Huber, Robust statistics, Wiley Series in Probability and Mathematical Statistics, J. Wiley & Sons, New York, Brisbane, Toronto, 1981.

[52] A. E. Beaton, J. W. Tukey, The fitting of power series, meaning polynomials, illustrated on band-spectroscopic data, Technometrics 16 (1974) 147–185.

[53] M. G. Kendall, A New Measure of Rank Correlation, Biometrika 30 (1/2) (1938) 81–93.

[54] C. Spearman, The proof and measurement of association between two things, American Journal of Psychology 15 (1904) 72–101.

[55] R. A. Fisher, Statistical Methods For Research Workers, Cosmo study guides, Cosmo Publications, 1925.

[56] S. S. Tripathy, R. Shekhar, R. S. Kumar, Texture retrieval system using intuitionistic fuzzy set theory, in: Proceedings of the 2011 International Conference on Devices and Communications, Jharkhand, India, 2011, pp. 1–5.